
*17th World Conference on Earthquake Engineering, 17WCEE*
*Sendai, Japan - September 13th to 18th 2020*

# FULL-SCALE TESTING OF CAST STEEL YIELDING CONNECTORS IN ACCORDANCE WITH AISC/SEI 41-13

J. Binder[1], M. Gray[2], C. Zhong[3], O. Kwon[4], C. Christopoulos[5],

[1] *Project Engineer, Cast Connex Corporation, j.binder@castconnex.com*
[2] *Executive Vice President, Cast Connex Corporation, m.gray@castconnex.com*
[3] *Graduate Researcher, Department of Civil and Mineral Engineering, University of Toronto, myron.zhong@mail.utoronto.ca*
[4] *Associate Professor, Department of Civil and Mineral Engineering, University of Toronto, os.kwon@utoronto.ca*
[5] *Professor, Department of Civil and Mineral Engineering, University of Toronto, c.christopoulos@utoronto.ca*

***Abstract***

The cast steel Yielding Connector (YC) is a steel component that is designed to dissipate earthquake energy through controlled flexural yielding of specially designed cast steel triangular fingers. The YC device is typically placed in series with a steel brace in a concentric braced frame and exhibits a stable hysteresis that precludes brace buckling. The YC connectors' small geometric size, large energy-dissipation capability, and ability to carefully control strength and stiffness during design make them promising devices for use as supplemental dampers in building retrofits or secondary seismic systems.

This paper presents the results of an experimental program wherein four full-scale YC designs (YC50, YC100, YC150, and YC215) were tested in accordance with the requirements of section 14 of the American Society of Civil Engineers (ASCE)/Structural Engineering Institute (SEI) Seismic Evaluation and Retrofit of Existing Buildings, ASCE/SEI 41-13. The four unique connector designs were each tested in both a brace test which had strictly axial deformations, and a subassemblage test in a reusable test frame which included in-plane brace rotations. Displacement protocols for each test were chosen using ASCE 41, with displacement magnitudes determined from an analysis of the low-cycle-fatigue capacity of the yielding fingers. Upon completion of the protocols, the devices were pushed to larger displacements in order to characterize device behavior under extreme conditions. For the subassemblage tests, a variety of brace and connection details were tested, including W- and HSS brace sections as well as both stiffened and unstiffened gusset plates.

The YC connectors all successfully passed the ASCE-41-13 protocols with minimal strength degradation, confirming their potential for use as supplemental energy dissipation devices. Upon pushing the devices to larger displacement levels beyond the AISC 41-13 protocols, the most common observed ultimate limit state was ultra low-cycle fatigue failure in the yielding fingers. Some failure modes were observed in the surrounding connection details, including sway-buckling in the unstiffened gusset-plate specimens. The observations of these limit states will help to inform the design procedure for the YC devices as they are used in supplemental damper configurations.

*Keywords: yielding, ductility, damper, energy dissipation*



## 1. Introduction

During the retrofit of seismically deficient structures, additional energy dissipation is often introduced to the building structure in order to improve seismic performance and control lateral deformations. This is achieved by the addition of energy dissipation devices in series with steel braces. Such devices are typically categorized as velocity-dependent devices, such as viscous dampers, or displacement dependent devices, such as friction or metallic yielding devices. These devices dissipate the applied earthquake energy and control the response of the building.

The Yielding Connector (YC) [1,2,3] is a novel steel component that was developed to act as a displacement-dependent yielding device for such retrofit situations. The YCs feature specially designed cast steel yielding fingers, which can undergo large displacement cycles before fracturing, and in turn absorb seismic energy. The YCs can be used in seismic retrofit projects to increase the ductility of any axially loaded members, and are typically placed in-line with a steel brace member. Alternatively, YCs can be used in the direction of the floor system, as shown in Figure 1a. YC devices have been previously tested in full scale testing [1,2] and as part of a suite of tests

This paper presents the results of an experimental program wherein four full-scale YC designs (YC50, YC100, YC150, and YC215) were tested in accordance with the requirements of section 14 of the American Society of Civil Engineers (ASCE)/Structural Engineering Institute (SEI) Seismic Evaluation and Retrofit of Existing Buildings, ASCE/SEI 41 [4] in order to confirm their adequacy with respect to their intended application in building retrofits.

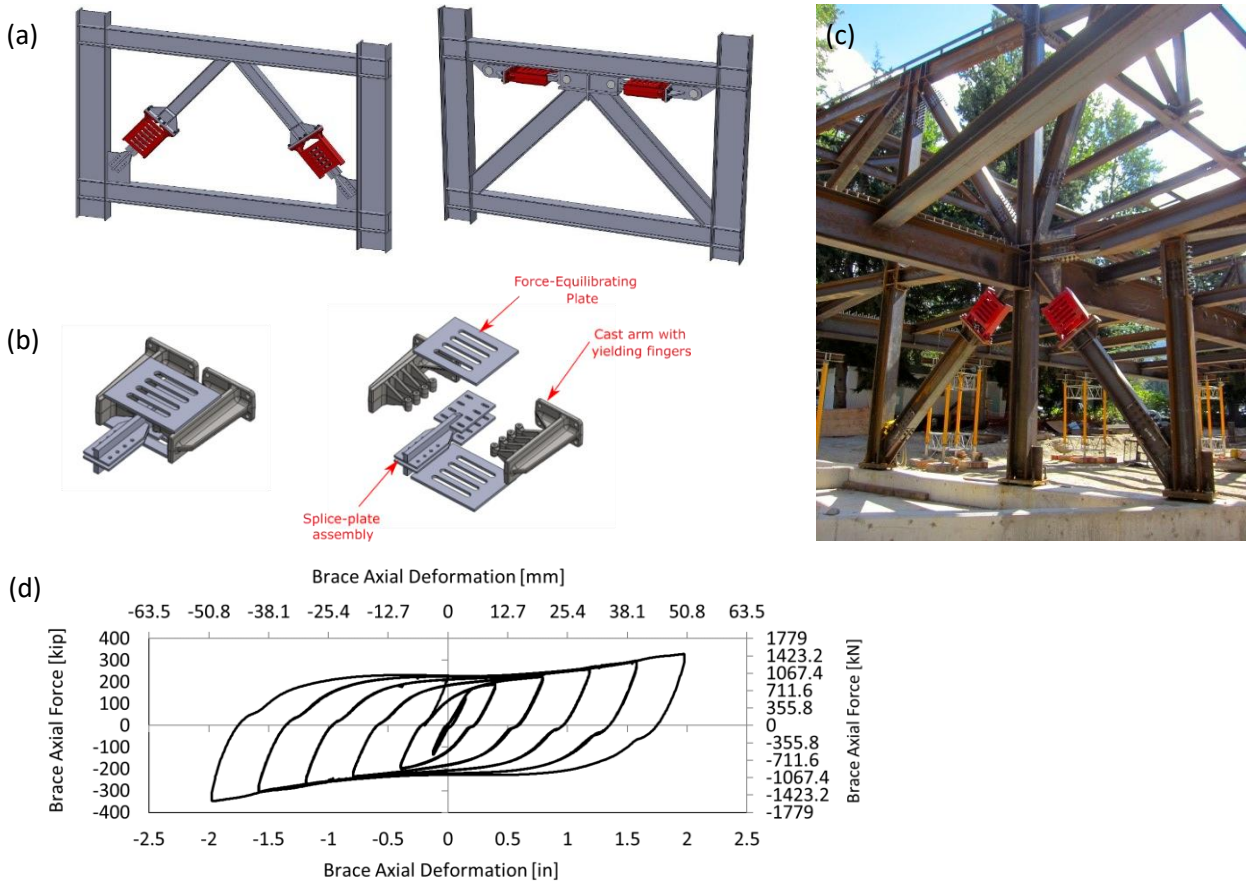


Figure 1: Overview of Yielding Connector; (a) Yielding Connectors oriented in-line with a concentric brace (left) and in the plane of the floor (right); (b) YC in a steel frame under construction; (c) schematic showing typical YC assembly including castings, cover plates, and splice plate assembly; (d) typical YC device hysteresis



 



## 2. Yielding Connector Overview

A schematic of a typical YC is shown in Figure 1b. The connector is comprised of two cast steel arms. The arms incorporate a series of triangular fingers that connect to a plate assembly (referred to as the splice plate assembly) via a structural bolt. The splice-plate assembly features holes that are slotted perpendicular to the primary axis of the device, thus allowing for the transfer for concentric forces without restricting the lateral motion of the end of the fingers (as is a typical requirement for adequate detailing of devices that incorporate triangular yielding fingers [5]). The two cast arms are connected by a pair of force-equilibrating plates which balance the bending moments induced by the yielding fingers. The end plates of the cast arms are in turn bolted to an end plate which is welded to a brace member. The splice-plate assembly is connected to other structural elements (such as a gusset plate) via a bolted or welded slotted-plate type connection.

Brace members can be W-section or Hollow Structural Section/Pipe. During design, brace members are selected using a capacity design approach where the compressive resistance of the brace is evaluated using AISC 360-16 [6] or a similar steel-design code. The brace member is typically governed by out-of-plane buckling, where the unbraced length is taken as the work-point-to-work-point length of the brace. The adjusted brace strength used in the design of the frame is calculated by multiplying the nominal connector strength (available in [7] by a factor, $\omega$, to estimate the strain hardening and post-yield stiffening and strengthening as well as a factor, $R_y$, to account for material yield strength variation. For design and frame analysis, the stiffness of the brace assembly is determined by combining the axial flexibilities of the brace and the connector. Figure 1c shows an example of how YC devices were incorporated into a typical steel frame building that used W-section steel braces.

Figure 1d shows a typical device hysteresis. The hysteresis features an increase in strength and stiffness at large displacements that is typical of triangular yielding fingers, due to tension that develops in the fingers under large deformations. This increase in strength and stiffness can be advantageous in reducing concentrations of inelasticity that can develop in multi-storey seismic systems that feature a low post-yield stiffness [8].

Since the YC devices feature multiple yielding fingers, a range of devices with a variety of strength and stiffness values is available by adding or subtracting pairs of yielding fingers. For example, the YC150 features ten yielding fingers and a nominal strength of 636 kN (143 kip), and is considered a device “parent”. “Child” devices are obtained by removing pairs of fingers from the parent in order to reduce the strength of the devices. For example, the YC120 device is identical to the YC150 except that it has eight fingers and a device strength of 509 kN (114 kip). All of the child devices feature identical yielding finger geometry to their parent, and thus their ductility capacity, which is based on the strain in the fingers as they deform in flexure, is theoretically the same for all identical fingers. Thus, the four “parent” devices were tested in this experimental program with an understanding that the test results will serve as validation of the behavior properties of the child devices as well. An overview of the entire range of available devices can be found in [7].

## 3. Experimental Setup

The devices that were tested were the YC50, YC100, YC150, and YC215. An overview of the devices, including nominal strength and stiffness, is given in Table 1. Each device was tested twice – once in a component test (Figure 2a), where the device was subjected to strictly axial deformations, and once in a subassembly test (Figure 2b), where the device was subjected to a combination of axial deformations and in-plane bending rotations. The subassemblage tests provided an opportunity to evaluate the YC connectors with respect to brace stability (brace and gusset plate buckling), and to confirm a variety of steel connection detail options.

The component tests consisted of a small brace stub, a YC device bolted to the brace stub, and a gusset plate connecting to the brace stub either via a bolted connection (YC100 and YC150) or a welded connection (YC50 and YC 215). An overview of the component tests, including photos of the specimens in the testing



 

frame (MTS 2700 kN axial testing machine) are shown in Figure 3, and an overview of the testing instrumentation is given in Figure 2a. Each specimen was instrumented with two string potentiometers on each side of the device and oriented in the brace axis that measured the axial deformation of the devices. Additional LED targets that interface with a 3D camera were used to capture 3D relative displacements. The cover plates of the YCs were instrumented with strain gauges. The testing machine measured brace axial force and machine head displacement.

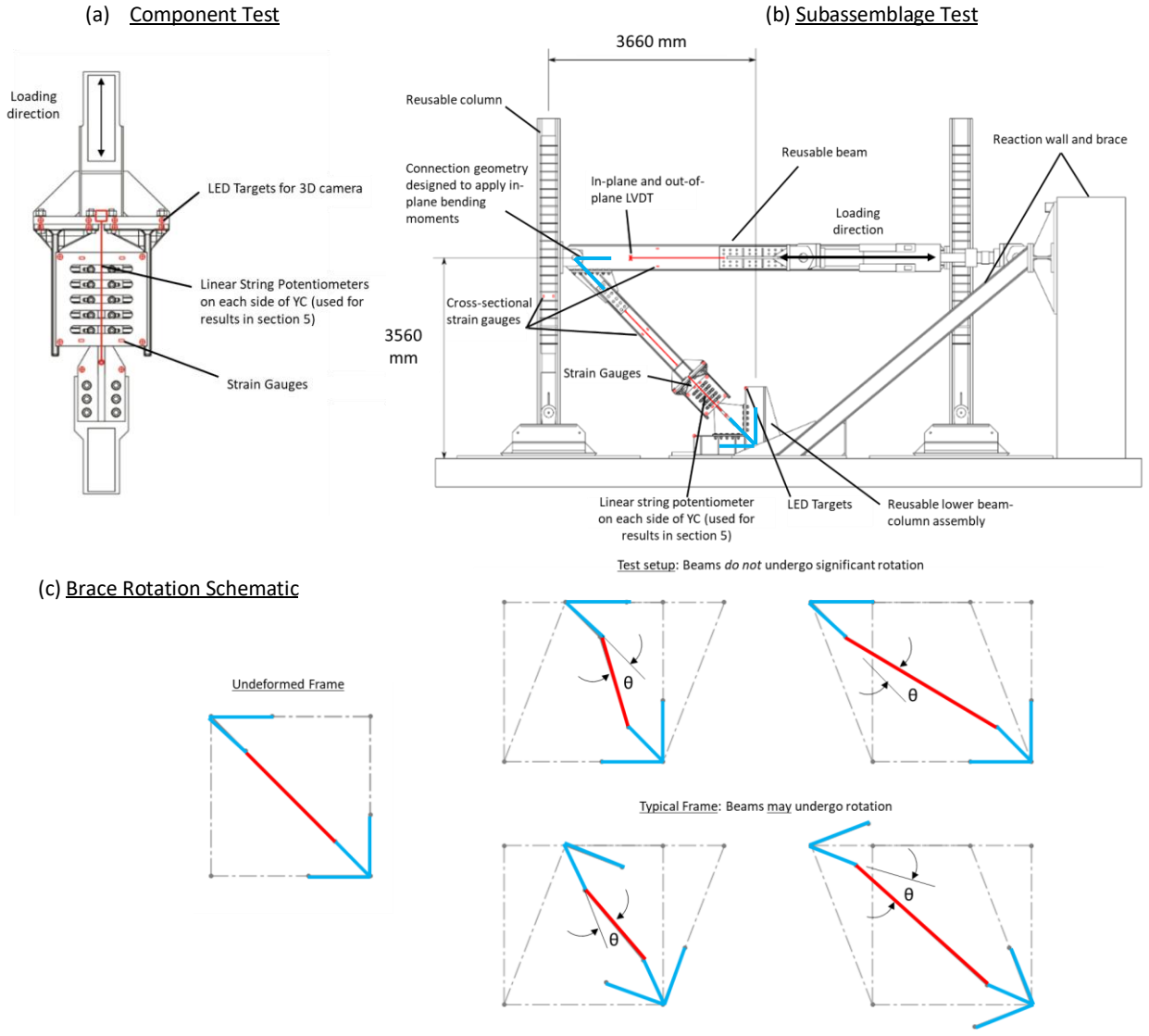


Figure 2: Overview of test setup and instrumentation; (a) component test; (b) subassemblage tests; (c) schematic of brace rotation demand in frame test as compared to a typical braced frame

Table 1: Overview of devices included in testing program

| Device | Nominal Strength | Nominal Stiffness |
|---|---|---|
| YC50 | 226 kN [50.8 kip] | 62.6 kN/mm [357 kip/in] |
| YC100 | 482 kN [108.4 kip] | 134.5 kN/mm [768 kip/in] |
| YC150 | 636 kN [143.0 kip] | 184.8 kN/mm [1055 kip/in] |
| YC215 | 932 kN [210 kip] | 209 kN/mm [1193 kip/in] |



 

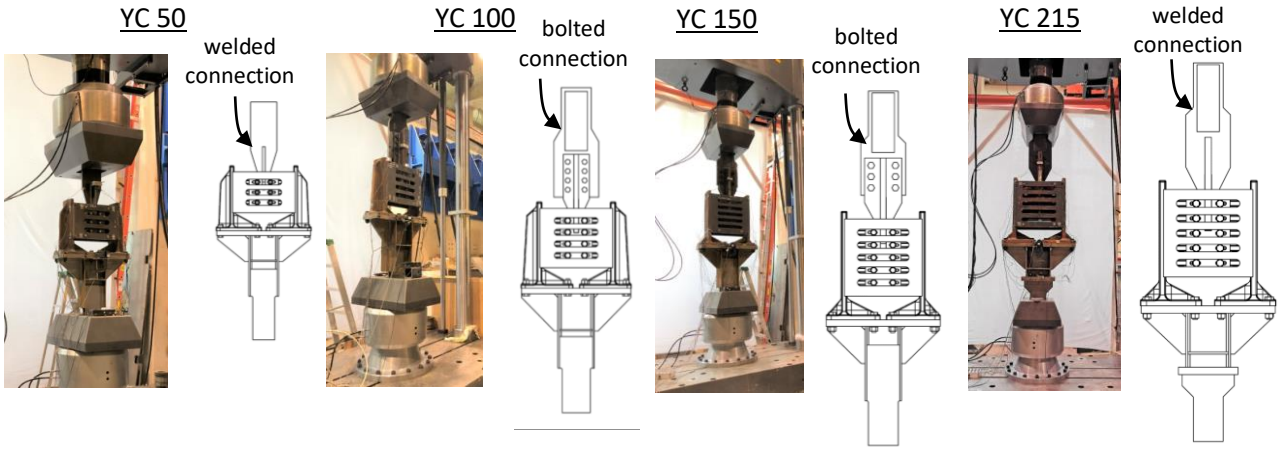


Figure 3: Overview of component tests

The subassemblage test specimens (shown in Figure 4) consisted of a lower gusset plate, YC device, brace member, and upper gusset plate. The lower gusset to splice plate assembly connections were bolted for the YC50 and YC215, and welded for the YC100 and YC150. Thus, between the component and subassemblage tests, each device was tested with both a bolted and welded lower gusset plate configuration. The upper gusset plate was bolted for all of the devices. All of the tests featured a W-section brace except for the YC100, which had a square HSS section brace. Accordingly, the connecting details between the YC100 and the HSS brace, and between the HSS brace and the upper gusset were somewhat different from the rest of the tests in that they made use of welded plates slotted into the HSS and bolted to the gusset via four angles. At the YC100 to HSS connection, welded stiffeners were used to ensure out-of-plane stiffness continuity to the device (shown in Figure 4). At the upper gusset plate connection, the bolted angles were used in a similar fashion.

The subassemblage test setup consisted of a reusable beam and column, as well as a reusable beam-column base assembly. The reusable beam was connected to the column with a true pin connection. Each subassemblage test specimen was then bolted to the beam above, and the beam-column assembly below. The manner in which this test setup imposes in-plane rotations on the braces if the beam flexural stiffness is significantly greater than that of the brace and brace-connection assembly, as compared to a typical frame where the beams above and below may experience rotations, is shown schematically in Figure 2c. In this case, the magnitude of the applied brace rotation shown schematically in Figure 2c as $\theta$, represents a conservative estimate of combined axial and in-plane flexural behavior of braces equipped with YC devices.

Further study of the bending brace bending moments including confirmation of the kinematic diagram shown in Figure 2c is given in [9], where finite element analysis results were used to study the experimental test setup brace-beam-column details as compared to typical steel details.

The YC50 subassemblage test featured unique lower and upper gusset plate details, in that they were designed with a free length of $2t_p$ thickness, where $t_p$ is the thickness of the gusset plate (shown in Figure 4 ). In this manner, these gusset plates were designed as they would be in a structure in which the braces are required to accommodate out-of-plane deformations. This free length is intended to limit the amount of out-of-plane flexural deformations in the brace and YC device by enabling hinging in the gusset plates on either ends of the brace. In contrast, the YC100, YC150, and YC215 do not feature this free length in their gusset plate details, and it is proposed that they will accommodate out-of-plane deformations by bending throughout the length of the brace, including the YC devices. While the scope of this testing program did not include the application of the out-of-plane deformations, the tests were intended to verify the variety of brace connection details presented herein with respect to the in-plane axial and rotational deformations that were applied. The design of the lower and upper gusset of the YC50 subassemblage test was undertaken to confirm an



 

appropriate design methodology for YC brace gusset plate connections. The performance of the details designed with this methodology is described in more detail in Section 5 of this paper.

The instrumentation scheme for the subassemblage tests is also shown in Figure 2b. These tests also feature string potentiometers on each side of the devices that measure the elongation of the devices. A variety of other sensors were used to capture brace elongation, strain in the braces, and frame deformation. Two actuators measured the applied story shear and actuator head displacement.

## 4. ASCE/SEI 41-13 Requirements and Displacement Protocols for Testing Program

ASCE/SEI Seismic Evaluation and Retrofit of Existing Buildings, ASCE/SEI 41-13 provides nationally applicable provisions for the seismic evaluation and retrofit of building structures. Section 14 of ASCE/SEI 41-13 presents suggested prototype testing for energy dissipation devices in order to confirm the nominal force versus displacement relations assumed in the seismic retrofit design. The requirements outline a loading protocol that consists of three separate test sequences; (a) ten cycles corresponding to 0.25 times the BSE-2X device displacement; (b) 5 cycles at 0.5 times the BSE-2X device displacement; and (c) three cycles at 1.0 times the BSE-2X device displacement, where BSE-2X is the device displacement associated with the maximum considered earthquake. The device must complete these three tests while maintaining an effective stiffness, $k_{eff}$ (defined in Section 14 of ASCE/SEI 41-13), maximum and minimum forces, and an area of the hysteresis loop $W_D$, that do not vary by more than plus or minus fifteen percent of the average of those values for all cycles in that test.

Table 2: Primary loading protocol for component and subassemblage tests, corresponding to requirements from ASCE 41-13

| **Device** | **$\Delta_y$** | **0.25×BSE-2X - 10 cycles** | **0.5×BSE-2X - 5 cycles** | **1.0×BSE-2X - 3 cycles** |
|---|---|---|---|---|
| YC50 | 2.42 mm (0.096 in) | 12.7 mm (0.5 in) | 25.4 mm (1.0 in) | 50.8 mm (2 in) |
| YC100 | 2.61 mm (0.103 in) | 14.3 mm (0.563 in) | 28.6 mm (1.123 in) | 57.2 mm (2.25 in) |
| YC150 | 2.56 mm (0.101 in) | 15.9 mm (0.625 in) | 31.8 mm (1.25 in) | 63.5 mm (2.5 in) |
| YC215 | 2.72 mm (0.107 in) | 15.9 mm (0.625 in) | 31.8 mm (1.25 in) | 63.5 mm (2.5 in) |

Table 2 gives the displacement protocols for component and subassemblage tests. These protocols were based on the qualification protocol in ASCE/SEI 41-13 described above. The displacement at which first yield occurs in the devices is given as well, for reference. The tests were controlled in both the component tests and subassemblage tests by the measured device elongation determined by averaging the two string potentiometers measurements. For each device the maximum achievable BSE-2X device displacement was determined using non-linear finite element analysis that incorporated a calibrated cyclic void growth model (reference [9,10,11]). A factor of 0.8 was applied to the low-cycle fatigue capacity in this model in order to ensure that the specimens would successfuly complete the protocol. The sequence of tests outlined in Table 2 is referred to herein as the “primary protocol”, since the primary aim of this testing program was to determine the devices’ ability to be used as a suplemental damper in the context of ASCE/SEI 41-13.

Once the devices completed the primary protocols described above, they were subjected to a “secondary protocol” in order to evaluate how the devices perform under a variety of extreme conditions. The secondary protocol for each device is outlined in Table 3. The determination of the secondary protocol varied for each device, and was chosen in order to investigate a variety of ultimate failure states.



 

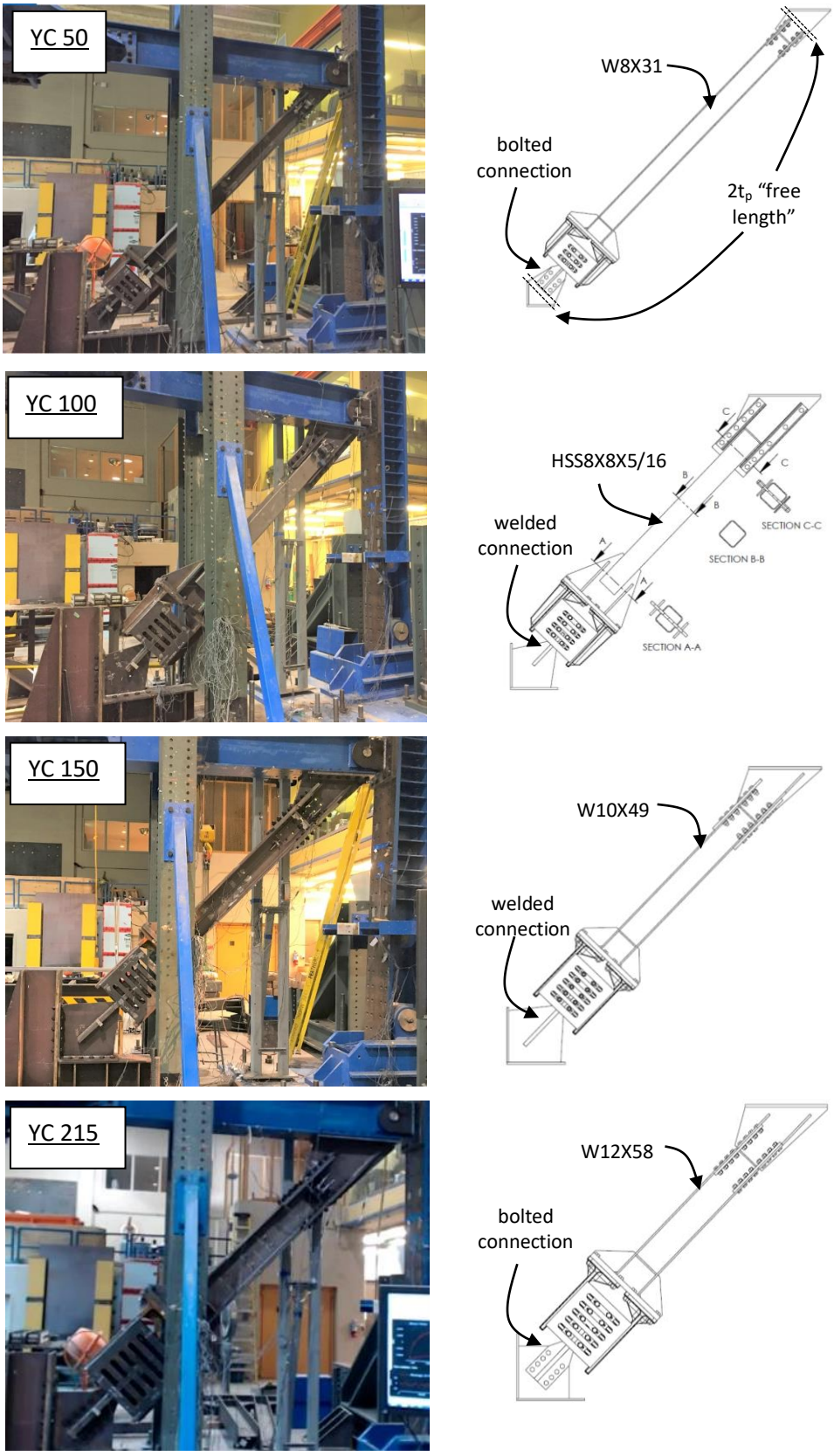


Figure 4: Overview of Subassemblage Tests



 

## 5. Testing Results

Figure 5 shows the hysteretic responses for the component and subassemblage tests. For the component tests, the results are presented as force versus displacement. The device force was determined from the testing machine actuator load cell, and the displacement was the YC device displacement calculated as the average of the string potentiometers located on each side of the devices. The subassemblage results are presented as storey shear versus frame drift. Here, the storey shear was determined from the frame actuator load cells, and the storey drift was estimated as the ratio of the story displacement to the story height, where the story displacement was measured as the average of the linear string potentiometers on each side of the YC devices divided by the cosine of the brace angle (46.1°)) to the story height, as shown in Figure 2b.

Table 3: Secondary loading protocol (extreme deformations) for component and subassemblage tests, including ultimate failure modes

| | Device | Secondary protocol (extreme deformations) | Failure modes |
|---|---|---|---|
| Component | **YC50** | • 2 cycles @ +/- 76.2 mm (3 in)<br>• 1 cycle @ +/- 82.6 (3.25 in)<br>• 3 cycles @ +/- 76.2 mm (3 in) | • ULCF* failure of yielding fingers |
| | **YC100** | • 2 cycles @ +/- 76.2 mm (3 in)<br>• 2 cycles @ +/- 82.6 mm (3.25 in) | • ULCF failure of yielding fingers |
| | **YC150** | • 1.5 cyces @ +/- 76.2 mm (3 in) | • Fracture of finger bolt (a)** |
| | **YC215** | • 0.25 cycles @ +/- 76.2 mm (3 in) | • Fracture of finger bolt (b) |
| Subassemblage | **YC50** | • 1 cycle @ +/- 76.2 mm (3 in)<br>• 2 cycles @ +76.2 mm (3 in), -82.6 mm (3.25 in)<br>• Monotonic pull in tension | • Buckling of upper gusset plate (c)<br>• Buckling of lower gusset plate (d)<br>• Fracture of finger bolts (e) |
| | **YC100** | • 3 cycles @ +/- 76.2 mm (3 in)<br>• Cycle to failure @ +/- 57.2 mm (2.25 in) | • ULCF failure of yielding fingers. |
| | **YC150** | • Cycle to failure @ +/- 63.5 mm (2.5 in) | • ULCF failure of yielding fingers |
| | **YC215** | • Cycle to failure @ +/- 76.2 mm (3 in) | • ULCF failure of yielding fingers |

* ULCF=Ultra Low-Cycle Fatigue
** letters correspond to hysteresis plots shown in Figure 5

The black lines in Figure 5 show the primary protocol adapted from ASCE 41-13. For all of the component and subassemblage tests, these black lines demonstrate the successful completion of these protocols, showing similar hysteretic behavior for all of the cycles within a given testing amplitude, and minimal strength degradation. The devices showed minimal visible signs of degradation (such as cracking in the yielding fingers) at the completion of this primary protocol. The results also demonstrated the similar behavior of the devices regardless of the presence of in-plane bending moments in the subassemblage configuration. The devices passed the requirements outlined in Section 14 of ASCE 41-13 with respect to effective stiffness, range of maximum and minimum force, and dissipation energy for each section of the loading protocol.

The grey lines in Figure 5 show the secondary protocol for each device. A description of the failure mode for each test is given in Table 3. For the YC50 and YC100 component tests, and the YC100, 150, and YC215 subassemblage test, the ultimate failure mode was ultra-low cycle fatigue (ULCF) in the yielding fingers. This failure mode is considered a desirable limit state for a device of this nature as it is not associated with a brittle collapse mechanism such as bolted connection fracture. Rather, ULCF failure happens gradually and the devices continue to dissipate significant energy even after significant strength degradation.

The YC150 and YC215 component tests experienced a fracture of the bolts that connect the YC cast steel yielding fingers to the splice plate assembly. At large deformations, the sliding action of the bolts



 

against the slotted holes of the splice plate assembly caused the bolt threads to cut into the bearing surface of the splice plate assembly and add to the bolt tension. These test results have informed design changes to the YC devices (including using a larger factor of safety in designing these finger bolts, as well as ensuring that the threads do not bear on the splice plate assembly) in order to prevent future bolt fractures. It is noted that the bolt fractures that were observed in these tests occurred after the completion of the primary protocols. No premature bolt fractures were observed in any of the other tests.

The YC50 subassemblage test, which was detailed with the "$2t_p$" free length in the lower and upper gusset plates, as described above, experienced a series of failure modes as the specimen was pushed to large displacements. The upper gusset plate was initially designed with an assumed free length of the average of $L_1$, $L_2$, and $L_3$ as shown in Figure 6. Along with an assumed effective length factor, K, of 1.0, this yielded a design strength $P_n$ of 1054 kN. Ultimately, the upper gusset plate buckled when the force in the brace (as estimated from the strain gauges attached to the brace) reached a value of 676 kN in compression at a displacement of -66 mm. This value is significantly lower than the value determined in the initial design, and thus the original design assumptions were unconservative. Upon reassessment of the design procedure used for the upper gusset plate, the guidelines put forth in [12] were considered, which recommends using the longest free length ($L_3$ in Figure 6) and an effective length factor of 1.2, so as to prevent the onset of sway buckling which can occur in braces with flexible gusset plates. Reference [12] states that "the relatively conservative value of 1.2 for K can be justified based on test results indicating that there is a possibility of end of bracing moving out of plane". Considering these new design parameters, the upper gusset plate design strength is 710 kN, which is consistent with experimental observation of 676 kN.

The upper gusset plate was replaced with an updated, thicker, design that considered the guidelines from [12], and the test was continued. After another displacement cycle, sway buckling of the brace occurred again, this time primarily due to the buckling of the lower gusset plate, shown in Figure 6. Again, the guidelines from [12] were helpful in explaining the observed experimental buckling value, as the experimental value at which buckling occurred, 761 kN, was very close to the value of 721 kN determined using K=1.2 and the longest free length of the gusset plate ($L_5$ in Figure 6).

After the lower gusset plate buckled in compression, the test was finished by monotonically pulling the frame to apply brace tension until fracture of the finger bolts occurred. This final monotonic pull in tension was useful in demonstrating how YC devices can achieve overstrength values in excess of 4.0 at large deformations, assuming there is sufficient ULCF life available in the fingers.



 

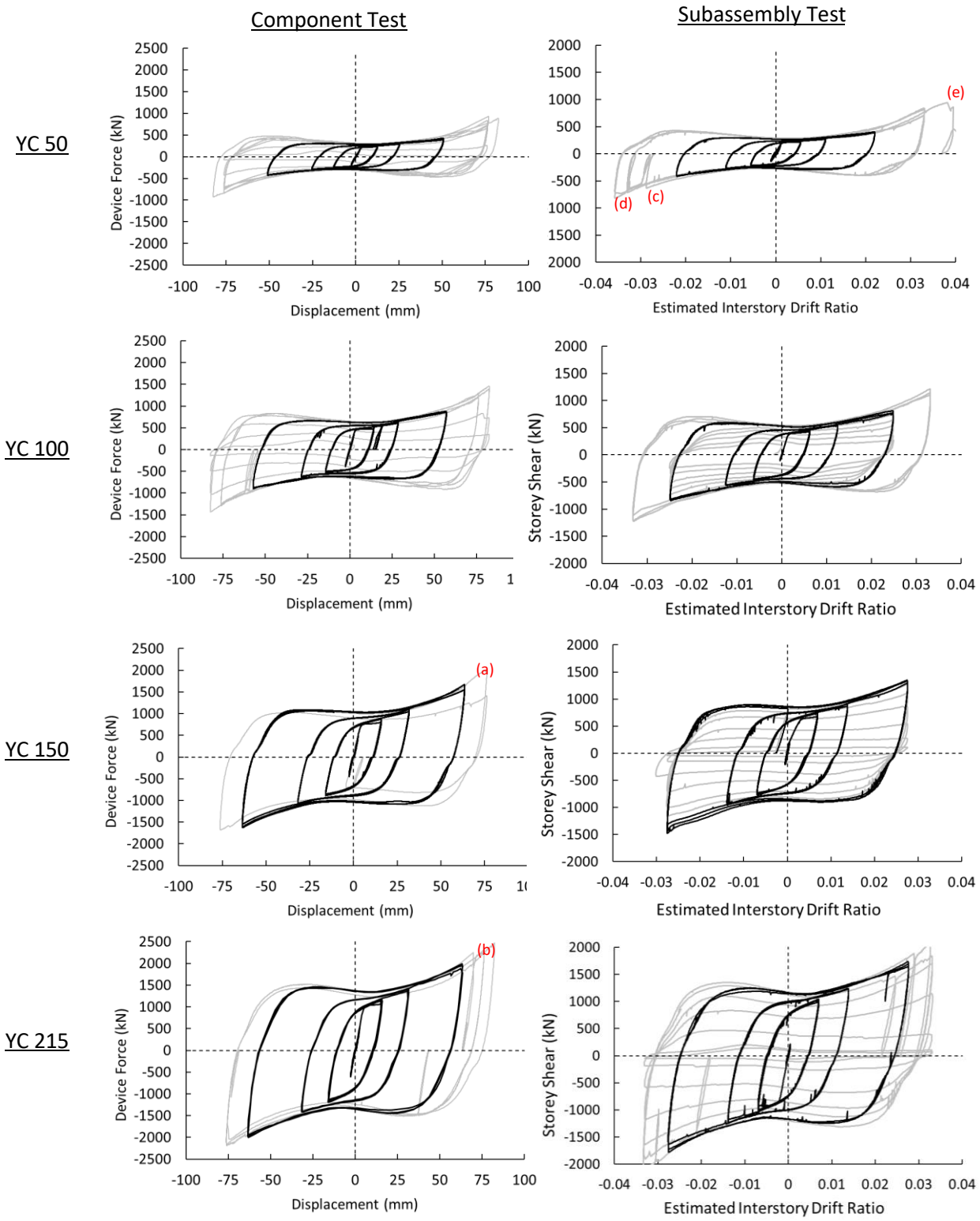


Figure 5: YC50 gusset plate performance at large frame deformations



 

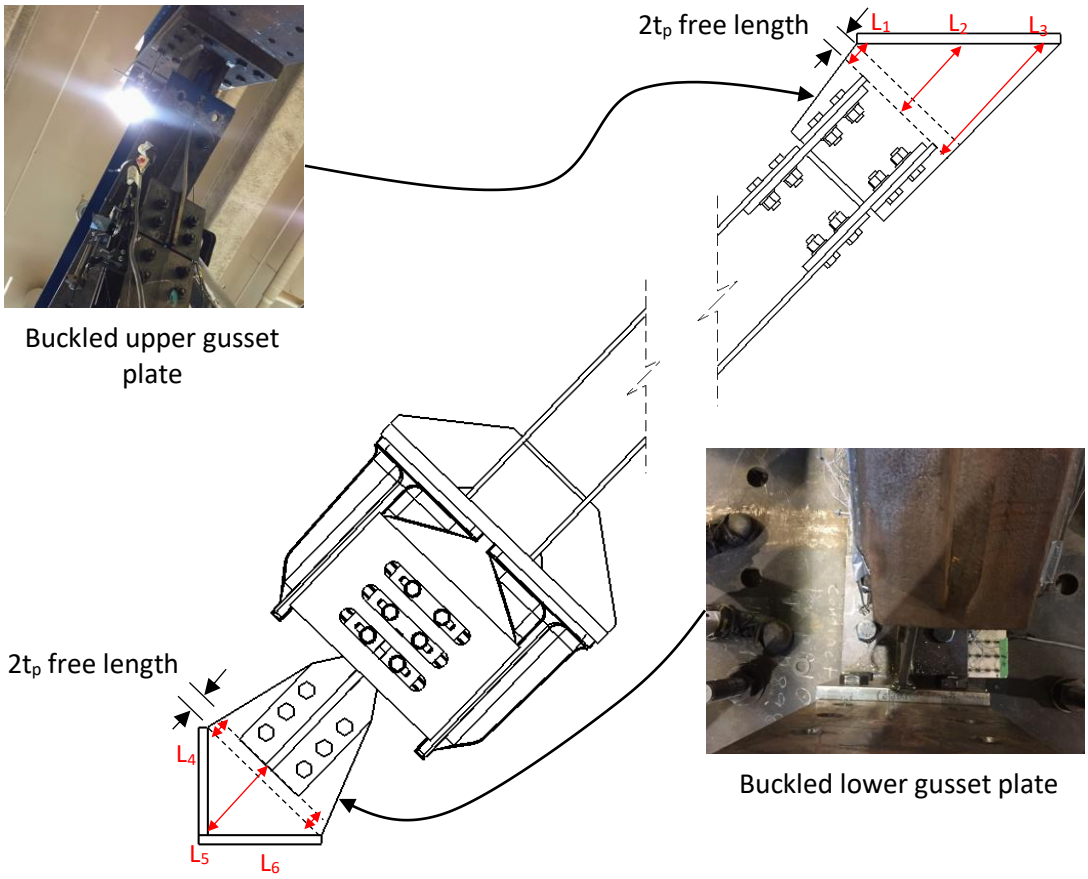


Figure 6: Buckling of YC50 subassemblage tests during large deformation excursions

## 6. Conclusions

This paper presented an overview of the results of an extensive experimental program on the Yielding Connector, a novel cast steel device that is intended to provide supplemental energy dissipation capacity in the retrofit of seismically deficient structures. In total, eight tests were performed on four unique YC device designs, and the following conclusions were drawn from the results:

- All of the YC devices successfully completed the inelastic protocol outlined in ASCE/SEI 41-13.
- The Subassemblage test results were not qualitatively different from the component test results, confirming that the presence of in-plane bending moments that are expected in a typical braced frame configuration does not appreciably affect the performance of the devices. Further discussion on these in-plane bending moments can be found in [9].
- Both bolted and welded connection details between the YC device and the gusset plate are suitable connection configurations.
- W-section and HSS-sections are suitable as braces in frames equipped with YC devices.
- Premature fracture of the bolts in the yielding fingers was observed in two of the tests at large displacements. While this failure mode is not expected to occur under design-level displacements, simple design changes to the YC device are proposed in order to eliminate this potential failure mode.
- When designing gusset plates that incorporate a "$2t_p$" free length, the guidelines from [12] are recommended in order to prevent frame sway buckling.



 

The results of this experimental program demonstrate that the YC device has high strength and large energy-dissipation capability even at large deformations. The YC device can be incorporated in steel braced frames with a variety of steel detailing configurations, and thus the devices are a promising option for use in the retrofit of seismically deficient structures.

## 4. Acknowledgements

The work would not be possible without the support of the Ontario Centres of Excellence (OCE) and the National Science and Engineering Research Council (NSERC), as well as the staff and technicians at the structural laboratory at the University of Toronto.

## 6. References

[1] Gray, M. G., Christopoulos, C., & Packer, J. A. (2014): Cast steel yielding brace system for concentrically braced frames: Concept development and experimental validations. *Journal of Structural Engineering*, **140**(4), 04013095.

[2] Gray, M. G., Christopoulos, C., & Packer, J. A. (2017): Design and full-scale testing of a cast steel yielding brace system in a braced frame. *Journal of Structural Engineering*, **143**(4), 04016210.

[3] Mortazavi, P., Kwon, O., Christopoulos, C., Gray, M. (2020): Four-Element Hybrid Simulation of a Steel Frame with Cast Steel Yielding Connectors. *17th World Conference of Earthquake Engineering*

[4] American Society of Civil Engineers (2013): ASCE/SEI 41-13. *Seismic Evaluation and Retrofit of Existing Buildings*

[5] Tsai, K. C., Chen, H. .W., Hong, C. P., & Su, Y. F. (1993): Design of steel triangular plate energy absorbers for seismic-resistant construction. *Earthquake Spectra* **9**(3), 505-528

[6] American Institute of Steel Construction (2016): ANSI/AISC 360-16. *Specification For Structural Steel Buildings*

[7] Gray, M. G., De Oliveira, J. C. (2020): Cast Connex Website. *https://www.castconnex.com*

[8] Gray, M. G., De Oliveira, J. C., Christopoulos, C., Binder, J. I. (2014): Effects of post-yield stiffening and strengthening on the collapse performance of non-buckling braced frames. *Tenth U.S. National Conference on Earthquake Engineering*

[9] Zhong, C., Binder, J., Kwon, O. S., & Christopoulos, C. (2020): Full-Scale Testing and Post-Fracture Simulation of the Cast Steel Yielding Connector. *Journal of Structural Engineering*. awaiting publication.

[10] Zhong, C., Binder, J., Kwon, O. S., & Christopoulos, C. (2020): Experimental and Numerical Characterization of Ultralow-Cycle Fatigue Behavior of Steel Castings. *Journal of Structural Engineering*, ***146***(2), 04019195.

[11] Smith, C. M., Deierlein, G. G., & Kanvinde, A. M. (2014): A stress-weighted damage model for ductile fracture initiation in structural steel under cyclic loading and generalized stress states. *Technical Rep, 187*.

[12] Astaneh-Asl, A. (1998) Seismic Behavior and Design of Gusset Plates. *Structural Steel Educational Council Technical Information and Product Service: Steel Tips*

[13] Mortazavi, P., Lee, E., Binder, J., Gray, M., Kwon, O., Christopoulos, C. (2020) Overview of Experimental Program on Cast-Steel Replaceable Yielding Links in Eccentrically Braced Frames. *17th World Conference on Earthquake Engineering*



 